

On Statistical Learning of Branch and Bound for Vehicle Routing Optimization

Andrew Naguib^{a,*}, Waleed A. Yousef^a, Issa Traoré^a, Mohammad Mamun^b

^aDepartment of Electrical and Computer Engineering, University of Victoria, 3800 Finnerty Road, Victoria, V8P 5C2, BC, Canada

^bNational Research Council, Fredericton, NB, Canada

Abstract

Recently, machine learning of the branch and bound algorithm has shown promise in approximating competent solutions to NP-hard problems. In this paper, we utilize and comprehensively compare the outcomes of three neural networks—graph convolutional neural network, GraphSAGE, and graph attention network—to solve the capacitated vehicle routing problem (CVRP). We train these neural networks to emulate the decision-making process of the computationally expensive Strong Branching strategy. The neural networks are trained on six instances with distinct topologies from the CVRPLIB and evaluated on eight additional instances. Moreover, we reduced the minimum number of vehicles required to solve a CVRP instance to a bin-packing problem, which was addressed in a similar manner. Through rigorous experimentation, we found that this approach can match or improve upon the performance of the branch and bound algorithm with the Strong Branching strategy while requiring significantly less computational time, even in comparison with the heuristic strategy referred to as the Reliable Pseudo-cost. The source code corresponding to our research findings and methodology is accessible and available for reference at the following web address: <https://isotlaboratory.github.io/ml4vrp>.

Keywords: branch and bound, combinatorial optimization, machine learning, transportation, logistics

1. Introduction

The capacitated vehicle routing problem (CVRP) (Dantzig and Ramser 1959) is a well-studied combinatorial optimization challenge with applications across diverse domains. It centers on the strategic allocation of a fleet of vehicles, all stationed at a common depot, to a set of customers with distinct demands. The primary objective is to facilitate a configuration of vehicle routes that minimizes the overall operational cost. When the vehicle fleet consists of a single unit, the CVRP reduces to the traveling salesperson problem (TSP).

Our study is focused on approximating solutions to the CVRP using graph neural networks (we shall expound on the details later in this section). Nevertheless, we would like to emphasize on the interrelation between the CVRP and the bin packing problem (BPP), a classic combinatorial problem in its own right. Remarkably, in situations where the travel expenses between customers are negligible (i.e., zero), the CVRP and BPP become equivalent. Furthermore, an intriguing parallel can be drawn between computing the minimal vehicle count required to attain feasible solutions within a CVRP instance and solving a bin packing problem—the primary reason for its integration into our work, which will obviate the need to “guess” the number or using a lower bound which is not necessarily feasible.

The CVRP and BPP are NP-hard problems (Lenstra and Kan 1981; Martello and Toth 1990). Exact solutions and approximate ones (Arora and Barak 2009; Papadimitriou and Yannakakis 1988) cannot be computed *efficiently* unless the $P = NP$ conjecture holds true. Heuristics with bounded-error ratios (Uchoa et al. 2017) are alternatively often used. Instead of using the general-purpose strategies, which are subject to performance limitations (Ho and Pepyne 2001), we spur the specialization of deep neural networks (especially the geometric ones) to specifically solve the CVRP and BPP rather than training an omniscient one. Statistical models possess the advantage of having a constant inference complexity. Moreover, the training time required for solving the CVRP or BPP is, as we shall demonstrate, negligible compared to the time needed to solve either deterministically.

We substitute the branching strategy of the branch and bound algorithm (B&B) (Land and Doig 1960) with one out of three graph neural networks. Then, we execute the solver and compare the duality gap between the native and trained branching strategies. To strengthen our analysis, we investigated the trained neural networks in a deterministically measurable environment, the mathematical solver SCIP (Bestuzheva et al. 2021).

The neural networks are trained on annotated samples of the decisions made by the strong branching strategy (SB) and compared against the reliable pseudo-cost strategy (RPC) (Applegate et al. 1995; Achterberg, Koch, and Martin 2005). The SB strategy (although computationally expensive) is guaranteed to obtain the optimum solution in the smallest B&B tree size. Hence, its decisions are efficient for training. Conversely,

*Corresponding author

Email addresses: ndrwnaguib@gmail.com (Andrew Naguib), wyousef@uvic.ca (Waleed A. Yousef), itraore@ece.uvic.ca (Issa Traoré), Mohammad.Mamun@nrc-cnrc.gc.ca (Mohammad Mamun)

the RPC branching strategy finds a suboptimal but high-quality solution in considerably less time, making it an ideal baseline for assessing temporal efficiency. We describe the intricacies of B&B algorithm as well as the SB and RPC strategies in Sections 2.3 and 2.4.

The combinatorial nature of the CVRP or BPP allows for numerous mathematical formulations. In this context, we adopt an integer programming perspective, which raises three fundamental questions:

- (A) How can graph neural networks be trained to approximate solutions for CVRP and BPP using an integer programming framework?
- (B) What trade-offs exist among solution quality, runtime, and training sample complexity?
- (C) How can we evaluate the generalization error of these approaches across various graph topologies that may differ from those encountered during training?

In response to question (A), we have devised two graph neural networks employing the architectures of the graph attention network (GAT) (Veličković et al. 2017) and the GraphSAGE model (Hamilton, Ying, and Leskovec 2017), while also assessing the graph convolutional neural network model (GCNN) proposed by (Gasse et al. 2019). Each of the three networks was trained on decision samples derived from the SB strategy while solving instances of the CVRP from the CVRPLIB (Lima et al. 2014) and the BPP from the Operation Research Library (Beasley 2004). We generated the decision samples by developing a fork of the École framework (Prouvost et al. 2020). Internally, École hooks events’ listeners on the solving process taking place inside of SCIP, the underlying mathematical solver.

As for question (B), we evaluated the efficacy of the classifiers established in (A) compared to the SB and RPC branching strategies. By conducting eight hundred experiments, we found that the classifiers consistently produced solutions that were either equivalent to, frequently superior to, or within a small fraction of the precision of the solutions derived from the SB or RPC, and in 2x-8x less time.

The challenge in (C) relates to delineating the concept of generalization error in our setup, which is distinct from the traditional approach of assessing the error using a sequestered test set. The accurate prediction of the branching variables in a test set by the classifiers does not unambiguously imply its ability to make valid decisions in instances of the CVRP with complex topologies. Thus, the question at hand is more challenging: How to measure the complexity of an integer program? Several factors require consideration, such as the instance topology, nature of the constraints, and number of binary variables. These factors also influence the estimated tree-size (TSE) of the B&B algorithm (Hendel et al. 2022; Özaltn, Hunsaker, and Schaefer 2011; Cornuéjols, Karamanov, and Li 2006), which we report in alongside with the graph edit distance (GED) (Abu-Aisheh et al. 2015) for each training and evaluation instance pair. We aim to establish a credible relation between the quality of solutions and complexity of the problem.

The rest of the manuscript is organized into different sections, beginning with Section 2, which provides an overview of the pertinent concepts employed in our research, followed by a literature review on the CVRP in Section 3. We elaborate on our approach in Section 4. We describe the experimental design in Section 5 and present the study’s results in Section 6. Finally, in Section 7, we discuss these results, the advantages and limitations of our method, and suggest potential avenues for future research.

2. Background

2.1. Integer Program

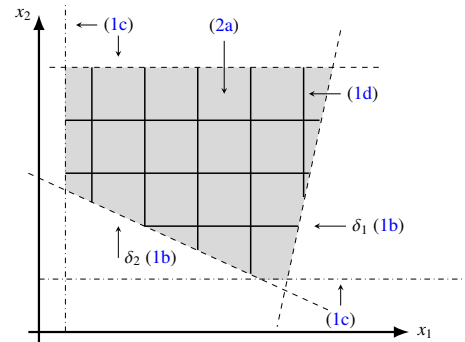


Figure 1: An IP example consisting of two variables and three constraints.

Let $x, c, l, u \in \mathbb{R}^n$, $A \in \mathbb{R}^{m \times n}$, $b \in \mathbb{R}^m$, $I \subseteq \{1, 2, \dots, n\}$, and $l, u \in \mathbb{R}^n$. An integer program (IP) can be defined as follows:

$$\underset{x}{\text{minimize}} \quad c^T x \quad (1a)$$

$$\text{subject to} \quad Ax \leq b, \quad (1b)$$

$$l \leq x \leq u, \quad (1c)$$

$$x_i \in \mathbb{Z} \quad i \in I. \quad (1d)$$

A *feasible* assignment $x_i = z_i$ must satisfy the above constraints (1b)-(1d), and an *optimal* one z^* , called the *minimizer*, is both feasible and minimizes the objective (1a). For a shorthand notation, let δ_i refer to $A_i x_i \leq b_i$ in (1b).

The *linear programming relaxation* (LP-relaxation) for the IP defined above would be:

$$\underset{x}{\text{minimize}} \quad c^T x \quad (2a)$$

$$\text{subject to} \quad Ax \leq b, \quad (2b)$$

$$l \leq x \leq u. \quad (2c)$$

That is, the integrality constraints are *relaxed*, which also makes the problem convex. The optimal solution to (2a) is also optimal to the original problem (1a) if and only if it satisfies (1d).

Figure 1 is an example of an integer program consisting of two variables, $\{x_1, x_2\}$, and two constraints, $\{\delta_1, \delta_2\}$. The gray shading represents the relaxed problem, (2a), where the solid grid lines are the integrality constraints, (1d), and the dashed lines, (1c), are the box constraints.

2.2. Primal-Dual Method

The quality of each feasible solution found to (1a) is assessed using the primal-dual method. The *primal (upper) bounds* p^* are provided by feasible solutions, and the *dual (lower) bounds* d^* by *relaxation* or duality. The Lagrangian dual problem (S. P. Boyd 2004 - 2004) to (2a) is:

$$\text{maximize}_{\lambda} \quad -b^T \lambda \quad (3a)$$

$$\text{subject to} \quad A^T \lambda + c \geq 0, \quad (3b)$$

where λ is the Lagrange multiplier or the dual variable for the inequality constraints (2b). The dual problem acts as a certificate on the limit of the performance, i.e., the upper bound that declares optimality of p^* . The duality gap f is given by $p^* - d^*$. A gap $f > 0$ or $f = 0$ indicates a *weak-* or *strong-*duality, respectively. We define the relative gap to be:

$$\Delta f = \frac{|p^* - d^*|}{\min\{|p^*|, |d^*|\}}.$$

In sequel, we shall drop the term “relative” and refer to Δf as gap.

2.3. Branch and Bound

The two building blocks in the algorithm are branching and bounding. In the branching step, the problem is divided into several smaller and less constrained ones and the bounding step selects which subproblems to solve next.

Formally, for a set of variables, $\{x_1, x_2, \dots, x_k\}$, the algorithm initializes the list of branching candidates $S = \{x_1\}$ (i.e., the first node), the optimal assignments $z_i^* = \phi$, and the optimal gap $f^* = -\infty$ (or any other heuristically known and feasible lower bound).

Then, (1) an LP-relaxation, LP_i (2a), is solved for the candidates in S (*bounding*), after which they are removed. (2) If the LP_i yields an infeasible solution $z_i \notin [l_i, u_i]$ and $S = \{\}$ (i.e., no more branching candidates), the algorithm halts. Otherwise, (3) another feasibility check is made to the *original* integer program (1a)-(1d), if $z_i \in \mathbb{Z}$ (1d), then $z_i^* = z_i$ and $f^* = f_{LP_i}$, which would then be an optimal solution. If $z_i \notin \mathbb{Z}$, (4) then sub linear programs LP_{i0}, \dots, LP_{in} are constructed from the current LP_i (*branching*) and whose union of the feasible-solution space does not contain z_i .

There are several strategies to drive the behavior of the branching and bounding steps (Morrison et al. 2016; Wosley 2020). A lower bound has not yet been proven for the algorithm and still an open question (Lipton and Regan 2012). The time required to solve a problem increases *exponentially* with the number of variables.

2.4. Strong Branching (SB) and Reliable Pseudo-Cost (RPC) Branching Strategies

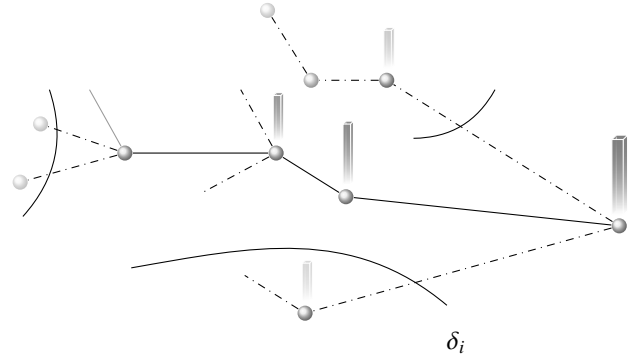


Figure 2: Illustration of the branch and bound process. The (*pruned*) dashed branches are depicted with arcs corresponding to a constraint δ_i . The superimposed bars represent the upper bounds.

The crux of SB is to carefully branch the tree to guarantee the smallest B&B tree size by performing a one-step lookahead before deciding to branch. The solver starts by choosing a set of integer variables, S , that are fractional in the LP-relaxation (when S represents all the integer variables, the strategy is called the Full Strong Branching). Then, temporal lower and upper bounds are calculated for the selected variable and upon which the subsequent paths are decided. In Figure 2, you can see a visual representation of the process. Each spherical node represents a variable, and the hovering bar shows its upper bound. The constraints, δ_i , play a role in deforesting the solution tree.

The SB strategy is commonly used in conjunction with other branching strategies to balance the trade-off between the solution quality and computational cost. On the other hand, the RPC branching strategy avoids the situation by assigning an estimated cost to each variable based on the results of the previous subproblems while occasionally using the SB strategy on the *unreliable* pseudo-costs according to a predefined reliability constant.

2.5. Capacitated Vehicle Routing Problem (CVRP)

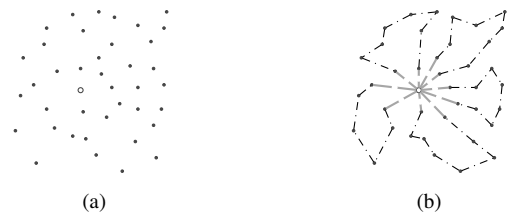


Figure 3: A CVRP example with $n = 40$ and $k = 5$. Given the dispersed points shown in (a), CVRP asks to find the routes presented in (b).

Let $G(V, \vec{A})$ be a *complete* graph consisting of the vertex set $V = \{0\} \cup N$ where $N = \{1, 2, \dots, n\}$ and the *directed* arcs set $\vec{A} = \{(i, j) : (i, j) \in V \times V, i \neq j\}$. There is a cost c_{ij} incurred for using an arc $a_{ij} \in \vec{A}$. For simplicity, we will assume that $c_{ij} = c_{ji}$. Each customer $i \in N$ has a nonnegative demand q_i .

The *out-degree* of a node is denoted by $\deg^+(i)$ for $i \in V$, that is, the number of arcs \vec{a}_{ij} leaving from node i to node $j \in V \setminus \{i\}$. Similarly, the *in-degree* of a node is denoted $\deg^-(v)$. At the depot $\{0\}$, there is a fleet of vehicles of size k with identical capacities Q . The goal is to construct a tour $\vec{T} \subseteq \vec{A}$ for each vehicle where

- (i) Each customer $i \in N$ is visited exactly once and by a single vehicle or tour T ;
- (ii) The demand served by tour \vec{T} does not exceed the capacity Q ;
- (iii) Each tour \vec{T} start and finish at the depot (to eliminate sub-tours);
- (iv) The constructed tours jointly minimize the total cost and serve the total demand $\sum_{i=1}^n q_i$.

The corresponding integer program is:

$$\text{minimize}_x \sum_{(i,j) \in \vec{A}} c_{ij} x_{ij} \quad (4a)$$

$$\text{subject to} \sum_{j \in \deg^+(i)} x_{ij} = 1 \quad \forall i \in V, \quad (4b)$$

$$\sum_{i \in \deg^-(j)} x_{ij} = 1 \quad \forall j \in V, \quad (4c)$$

$$\sum_{j \in \deg^+(0)} x_{0j} = k, \quad (4d)$$

$$\sum_{j \in \deg^-(0)} x_{0j} = k, \quad (4e)$$

$$u_i - u_j + Qx_{ij} \leq Q - q_j \quad \forall (i, j) \in \vec{T}, \quad (4f)$$

$$q_i \leq u_i \leq Q \quad \forall i \in N, \quad (4g)$$

$$x_{ij} \in \{0, 1\} \quad \forall (i, j) \in \vec{A}, \quad (4h)$$

where $x \in \mathbb{Z}^{|\vec{V}| \times |\vec{V}|}$ and $u \in \mathbb{R}^{|\vec{T}|}$ are the decision variables representing the arc set \vec{A} and constructed tour \vec{T} , respectively. The equations (4b) and (4c) stipulate constraint (i). The sub-tour elimination and capacity constraints (SEC), which correspond to constraints (ii) and (iii), are guaranteed by (4f) and (4g). These equations are the Miller-Tucker-Zemlin (MTZ)-formulation of SEC (C. E. Miller, Tucker, and Zemlin 1960). The integrality constraints are enforced by equation (4h).

2.6. Bin Packing Problem (BPP)

Formulating an IP for the BPP in terms of the CVRP can be written by removing constraints (4f)-(4g) and through a simple algebraic manipulation to minimize the number of vehicles, referred to as bins in this context, in lieu of (4a). We achieve so by expanding the value k to the *bins* variable $K = \{1, 2, \dots, k\}$, and restricting that the demands $q_j \forall j \in N$, represented as weighted items, must be distributed across the available bins without exceeding the bin's capacity Q .

$$\text{minimize}_k \sum_i^k k_i \quad (5a)$$

$$\text{subject to} \sum_i^k q_j x_{ij} \leq Qk_i \quad \forall j \in N, \quad (5b)$$

$$\sum_i^k x_{ij} = 1 \quad \forall j \in N, \quad (5c)$$

$$k_i \in \{0, 1\} \quad \forall i \in K, \quad (5d)$$

$$x_{ij} \in \{0, 1\} \quad \forall i \in K, j \in N. \quad (5e)$$

The decision variable x represents the allocation of customers' demands or items to vehicles or bins, with each entry $x_{i,j}$ representing the assignment of the i -th vehicle or bin to the j -th demand or item.

We reformat equation (5b) as $\sum_i^k q_j x_{ij} - Qk_i \leq 0$ to match the format required by a SCIP constraint. The solution to this integer program, let it be denoted k_{\min} , replaces the value of k in (4f)-(4g), which is frequently set to be the strict lower bound calculated as $\lceil \frac{\sum_i^n q_i}{Q} \rceil$ —however, this lower bound is not necessarily feasible. The equation(s) (5b) represents the bin capacity constraint, (5c) ensures that each item is assigned to a single bin, and (5d)-(5e) are the integrality constraints.

3. Literature Review

Solving optimization problems by using neural networks emerged from the work of (Hopfield and Tank 1985), who formulated the TSP as an energy minimization problem and showed that the energy function decreases as the algorithm (a neural network) progresses to a local optimum; that said, it was still behind several heuristics. Attempts to utilize the same idea for CVRP were first examined by (Torki, Somhon, and Enkawa 1997; Ghaziri 1996). Although the internals of the two approaches differ, they both employ self-organizing feature maps and show on-par performance with other heuristics such as (Clarke and Wright 1964; Gillett and L. R. Miller 1974). Building a search tree based on the branch and bound algorithm has remained a promising approach for decades and many studies have contributed to guiding heuristics and branching policies.

The effectiveness of using a machine learning model to imitate the decisions of the B&B algorithm by replacing the underlying branching policy was first studied by (Khalil et al. 2016). They trained a surrogate function to rank the decisions collected from the SB branching policy, treating it as a learning-to-rank problem. Their results showed promise for this approach. Later, (Gasse et al. 2019) used deep neural networks to further improve this idea, formulating the B&B as a Markov decision process and evaluating it on four NP-hard problems: set cover, capacitated facility location, combinatorial auction, and maximum independent set. Notably, (Nair et al. 2020) were able to build on this work and develop a batch LP-solver that generates 2.6 times more data samples than its sequential counterpart—the underlying theoretical framework is alternating direction

elements into latent vectors $H_\delta \in \mathbb{R}^{m \times d}$, $H_A \in \mathbb{R}^{m \times n \times d}$, and $H_x \in \mathbb{R}^{n \times d}$, where d is the embedding dimension.

The transformation module for δ and x , includes a layer normalization (LayerNorm, as proposed by (J. L. Ba, Kiros, and Hinton 2016)), linear transformation, and rectified linear unit (ReLU) as the nonlinearity, which we denote as σ . For convenience, we construct f to embed the elements $i \in H_x$ and $j \in H_\delta$ as follows:

$$f(y) = \begin{cases} y, & \text{if } l = 0 \\ \sigma(W^{(l)} \text{LayerNorm}(y)), & \text{otherwise} \end{cases} \quad (6)$$

$$H_x^{(0)} = \{ \underbrace{f(x_1)}_{h_{x_1}^{(0)}}, \underbrace{f(x_2)}_{h_{x_2}^{(0)}}, \dots, \underbrace{f(x_n)}_{h_{x_n}^{(0)}} \}, \quad (7)$$

$$H_\delta^{(0)} = \{ \underbrace{f(\delta_1)}_{h_{\delta_1}^{(0)}}, \underbrace{f(\delta_2)}_{h_{\delta_2}^{(0)}}, \dots, \underbrace{f(\delta_m)}_{h_{\delta_m}^{(0)}} \}, \quad (8)$$

where $W^{(l)}$ is a weights matrix at layer (l), and is distinctive among the ensuing expressions. For the transformation of A , only the LayerNorm is used:

$$H_A^{(0)} = \underbrace{\text{LayerNorm}(A_{ij})}_{h_{A_{ij}}}, \quad \forall (i, j) \in A. \quad (9)$$

The authors apply a custom graph convolution to the produced the latent vectors in two phases. In the first phase, they convolve over the triplet (H_x, H_A^T, H_δ) to compute Message $m_{(ij)}^{(l)}$, which is the convolution on the constraints side, that is represented as $C_{x-\delta}$. This convolution is calculated as follows:

$$h_{ij}^{(l)} = W^{(l)} h_{x_i}^{(l-1)} + W^{(l)} h_{A_{ij}}^{(l-1)} + W^{(l)} h_{\delta_j}^{(l-1)}, \\ \bar{h}_{ij}^{(l)} = \text{LayerNorm}(W^{(l)}(\sigma(W^{(l)} h_{ij}^{(l)}))).$$

In this step, the effect of each variable on the constrained region is learned. The AGGREGATE operation is defined as reduction by summation of all normalized features from the neighboring nodes in the set δ , which is referred to as Message m_{ij} :

$$\text{AGGREGATE}^{(l)}(H_x, H_A, H_\delta) = \sum_{j \in \mathcal{N}(i)} \underbrace{\bar{h}_{ij}^{(l)}}_{m_{ij}^{(l)}}, \quad (10)$$

$$C_{x-\delta}^{(l)} = \text{UPDATE}^{(l)}(\{i \in |H_x|\}) = W^{(l)} h_{x_i} + W^{(l)}(m_{ij}^{(l)}).$$

$\mathcal{N}(i) = \{j | A_{ij} \neq 0 \forall j \in |A_i|\}$ is the set of neighboring nodes and $|\cdot|$ is the cardinality operator. In the second phase, the same operations are used. However, to convolve over the triplet $(C_{x-\delta}, A, x)$, a similar concept of learning is performed from the side of the constraints, C_δ , against the previously produced variable convolution. This process is defined as follows:

$$C_{\delta-x}^{(l)} = \text{UPDATE}^{(l)}(\{i \in |H_\delta|\}) = W^{(l)} h_{\delta_i} + W^{(l)}(C_{x-\delta}^{(l)}). \quad (11)$$

Eventually, log probabilities over possible branching candidates are estimated by a nonlinear transformation of the resulting convolution $C_{\delta-x}$, and the branching candidate has the highest log probability:

$$\hat{v} = \text{argmax}(W^{(l+1)}(\sigma(W^{(l+1)} C_{\delta-x}^{(l)}))). \quad (12)$$

4.2. GraphSAGE

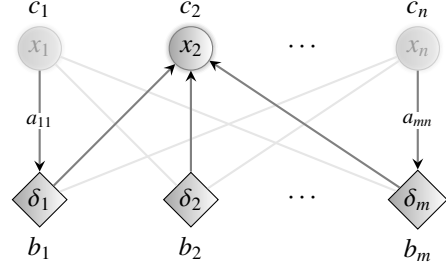


Figure 5: GraphSAGE accumulates information from a selection of neighboring nodes, with more distant nodes becoming increasingly influential in the aggregated information as the process continues.

The inputs to the nonbipartite deep graph neural networks are curated differently; the constraints $\delta_{n \times 5}$ are first padded with zeros to match the variable row dimension, resulting in $\delta_{m \times 19}^{pad} = [\delta_{m \times 5} \mathbf{0}_{m \times 14}]$. Then, the variables $x_{n \times 19}$ and the padded constraints $\delta_{m \times 19}^{pad}$ are augmented to form the input $H = \begin{bmatrix} x_{n \times 19} \\ \delta_{m \times 19}^{pad} \end{bmatrix} \in \mathbb{R}^{(n+m) \times 19}$, which is then fed en bloc to the classifier. The adjacency matrix would then be a zero-diagonal matrix with the coefficients being off-diagonal¹:

$$\mathbf{A} = \begin{bmatrix} \overbrace{\begin{matrix} 0 & \cdots & 0 \\ \vdots & \ddots & \vdots \\ 0 & \cdots & 0 \end{matrix}}^n & \overbrace{\begin{matrix} a_{11} & \cdots & a_{1m} \\ \vdots & \ddots & \vdots \\ a_{n1} & \cdots & a_{nm} \end{matrix}}^m \\ \overbrace{\begin{matrix} a_{11} & \cdots & a_{1n} \\ \vdots & \ddots & \vdots \\ a_{m1} & \cdots & a_{mn} \end{matrix}}^n & \overbrace{\begin{matrix} 0 & \cdots & 0 \\ \vdots & \ddots & \vdots \\ 0 & \cdots & 0 \end{matrix}}^m \end{bmatrix} \\ = \begin{bmatrix} \mathbf{0} & A \\ A^T & \mathbf{0} \end{bmatrix}.$$

We start by taking a linear transformation of the inputs to produce $H' \in \mathbb{R}^{(n+m) \times 19 \times d}$:

$$H^{(0)} = \begin{bmatrix} \underbrace{W^{(0)} x_1}_{h_1^{(0)}}, \dots, \underbrace{W^{(0)} x_n}_{h_n^{(0)}}, \underbrace{W^{(0)} \delta_1}_{h_{n+1}^{(0)}}, \dots, \underbrace{W^{(0)} \delta_m}_{h_{n+m}^{(0)}} \end{bmatrix}, \quad (13)$$

¹The matrix can be constructed and stored efficiently using coordinate format.

where $W^{(l)} \in \mathbb{R}^{d \times 19}$. The message produced for Node $i \in H'$, denoted m_i , is defined as:

$$m_i^{(l)} = \text{AGGREGATE}^{(l)}(h_i) = \underbrace{\frac{1}{|\mathcal{N}(i)|} \sum_{j \in \mathcal{N}(i)} h_j^{(l)}}_{\text{Neighborhood Averaging}}, \quad (14)$$

$$\text{UPDATE}^{(l)}(\{\forall i \in |H^{(l)}|\}) = \sigma \left(W^{(l)} h_i + W^{(l)} m_i^{(l-1)} \right),$$

where $\mathcal{N}(i) = \{j | A_{ij} \neq 0, \forall j \neq i \in |H'|\}$. Log probabilities over the branching candidates are obtained by a linear transformation over the updated features. The branching candidate is then selected using:

$$\hat{v} = \text{argmax} \left(W^{(l+1)} H^{(l)} \right) \quad (15)$$

4.3. Graph Attention Network (GAT)

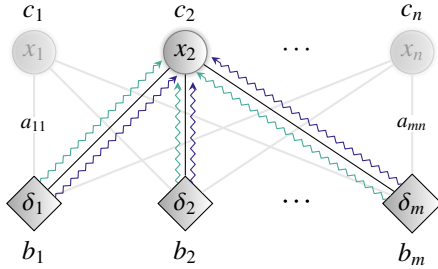


Figure 6: GAT assigns attention scores to the relationships between each node and its neighboring nodes. This is an example of a three-head attention mechanism.

The input to the GAT is the same as the input to GraphSAGE, H . Similarly, H' is computed using Equation (13). We then train a self-attention mechanism, denoted as $a : \mathbb{R}^d \times \mathbb{R}^d \rightarrow \mathbb{R}$, defined as:

$$a^{(l)}(h'_i, h'_j) = \text{LeakyReLU} \left(w_a^{T(l)} \odot \left[h'_i \parallel h'_j \right] \right),$$

where $\text{LeakyReLU}(y) = \max(0, y) + m \cdot \min(0, y)$, $w_a^{T(l)} \in \mathbb{R}^{2d}$, and \parallel represents the concatenation operator. The attention score α_{ij} is then generated by normalizing the attention coefficients assigned to the neighboring nodes using a with the softmax function and multiplying by \mathbf{A}_{ij} in the following way:

$$\alpha_{ij}^{(l)} = \frac{\exp(a^{(l)}(h_i, h_j))}{\sum_{j \in \mathcal{N}(i)} \exp(a^{(l)}(h_i, h_j))} \odot \mathbf{A}_{ij}.$$

Such a score indicates the learned connectivity strength of Node i to Node j rescaled by the decision variable coefficient. The AGGREGATE operation performs a nonlinear combination of the learned attention scores and the linearly transformed inputs:

$$\text{AGGREGATE}^{(l)}(i) = \sigma \left(\sum_{j \in \mathcal{N}(i)} \alpha_{ij} h'_j \right).$$

The nonlinearity, σ , is used to prevent unintended fluctuations in the learned attention values. To integrate a K -head attention mechanism, for $K \in \mathbb{Z}^+$ (see Figure 6), the outputs are averaged among K independent operators, and the message-protocol is constructed by:

$$m_i^{(l)} = \frac{1}{K^{(l)}} \left(\sum_{k=1}^{K^{(l)}} \text{AGGREGATE}^{(l)}(h_i) \right) \quad (16)$$

$$\text{UPDATE}^{(l)}(\{\forall i \in |H^{(l)}|\}) = \sigma \left(W^{(l)} h'_i + W^{(l)} m_i^{(l-1)} \right).$$

The branching candidate is decided, analogously to GraphSAGE, by:

$$\hat{v} = \text{argmax} \left(W^{(l+1)} H^{(l)} \right) \quad (17)$$

5. Experiments

The SB decision samples were drawn using École by formulating the CVRP and BPP as outlined in Sections 2.5 and 2.6, respectively. The CVRP training and evaluation instances were drawn from CVRPLIB (Lima et al. 2014), with six instances from sets A and P (P et al. 1995) for training (A-n32-k5, A-n33-k5, A-33-k6, A-n39-k5, A-n44-k6, and P-n40-k5) and eight instances from sets P, B, and M for evaluation: (P-n76-k5, P-n60-k15, P-n65-k10, B-n78-k10, B-n64-k9, B-n57-k7, M-n101-k10, and M-n151-k12). Each instance comprises of the following attributes: the number of customers, the demand of each customer, and the location of the depot and customers in a two-dimensional Euclidean space, where the cost c_{ij} in (4a) corresponds to the Euclidean distance between node i and node j .

Similarly, the BPP training instances were selected from (Beasley 2004), specifically sets U and T, with two instances for training (u100_00 and u80_00) and five instances for evaluation (t249_00, t120_00, t60_00, u250_00, and u500_00)

The training and evaluation instances are referred to as **tr** and **ts**, respectively. The configuring parameters in SCIP were set to their default, except for disabling the separation routine, enabling the search-tree-size profiling, and the branching strategy idempotence.

5.1. Training

Due to the computational cost imposed by SB, we randomly set the strategy to either the RPC or SB at each branching. But, we only exported the branchings decided by the SB strategy to the training dataset. The size of which, denoted as N , is 10^5 for each sampled dataset $\mathcal{D} = \{(x_i, A, \delta_i, v_i)\}_{i=1}^N$, where each record is an independent and identically distributed sample from the SB decisions.

The classifiers were trained to maximize the log likelihood (Pawitan 2013) using adaptive stochastic gradient ascent (Kingma and J. Ba 2014):

$$\mathcal{L}(\hat{v}, v) = \frac{1}{N} \sum_{i=1}^N \log \pi_{\theta}(\hat{v}_i = v_i | x_i, \delta_i). \quad (18)$$

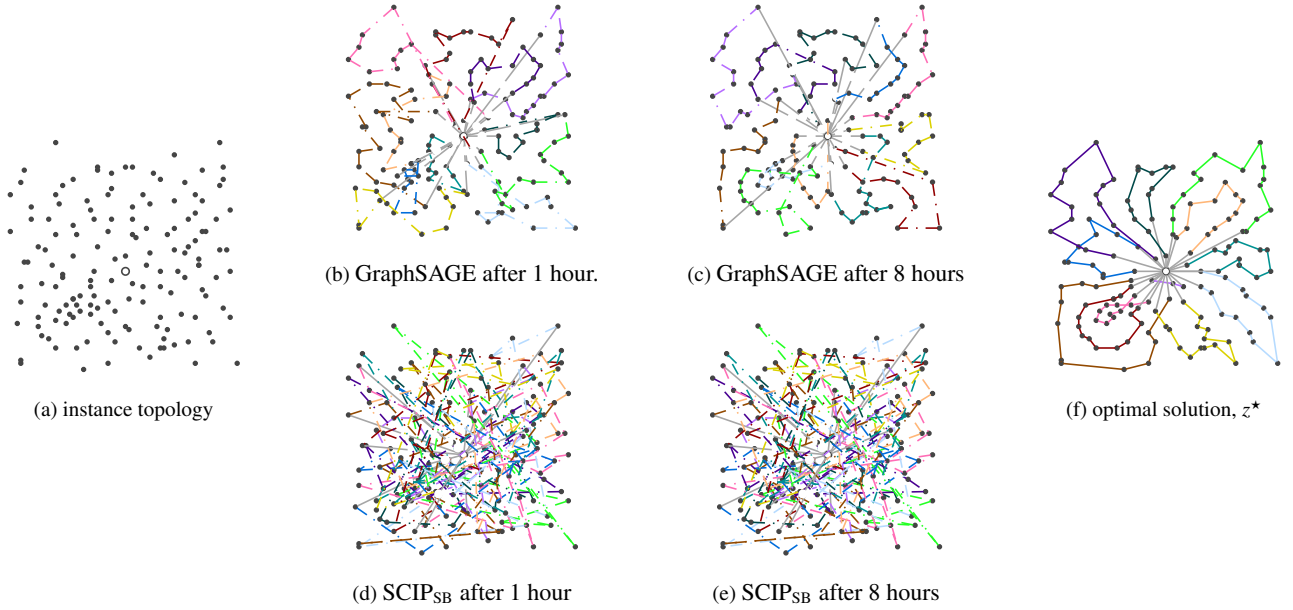


Figure 7: Example on solving Instance M-n151-k12 using both GraphSAGE and SCIP with allowed runtime of 8 hours.

A verbal explanation of equation (18) is: given a set of constraints δ_i , the variable features x_i , and the decided branching variable v_i , we aim to maximize the likelihood that a classifier, or policy, π parameterized by the weights θ selects the same branching decision, \hat{v}_i , using either (12), (15) or (17).

At each iteration, we tested the performance on a sequestered validation set. We did not use dropout or add self-loops. The tuning parameters of each classifier are set to the following values:

- GCNN: $d = 64$, $l = 1$, $m = 0.2$;
- GraphSAGE: $d = 64$ and $l = 5$;
- GAT: $d = 128$, $l = 2$, $K_1 = 2$, and $K_2 = 4$.

These values were chosen through an experiential process that targeted minimizing the empirical *training* error (to prevent an overuse of the validation sets (Hastie, Tibshirani, and Friedman 2009; Feldman, Frostig, and Hardt 2019; Mania et al. 2019)).

5.2. Evaluation

We evaluated five branching strategies: SB, RPC (which are the inherently built branching strategies), GCNN, GraphSAGE, and GAT (which are the learned strategies) using SCIP with the time limit set to 1 hour, 2 hours, 4 hours, or 8 hours when solving each evaluation instance $j \in \mathbf{ts}$. For brevity, the gap achieved by SCIP using the SB or RPC strategies will be referred to as SCIP_{SB} and SCIP_{RPC} , respectively. We also use the notation SCIP_s to refer to either of them. In Figure 7, we contrast the solution quality obtained by GraphSAGE against that of SCIP_{SB} on the first (see Figures 7b and 7d) and eighth (see Figures 7c and 7e) hours when solving the CVRP instance M-n151-k12 (see Figure 7a). As shown, there is a strong resemblance between the constructed tours and the optimal ones

(see Figure 7f) only after a single hour of execution. However, we shall introduce solid assessment metrics.

We define the optimality gain using a four-faceted comparison. Let $\Delta f_{j,t}^{\text{SCIP}_s}$ be the gap of SCIP using the strategy s on \mathbf{ts}_j , which is the j -th instance of \mathbf{ts} , after t hours of solving. We let $\Delta f_{j,t}^{m_i}$ be the gap of model m when trained on \mathbf{tr}_i , which is the i -th instance of \mathbf{tr} , and evaluated on \mathbf{ts}_j after t hours of solving. Then, we assess the quality of our proposed approach by calculating the following relative performance measure:

$$\Delta f_{\text{SCIP}_s}^m(i, j, t, k) = \frac{\Delta f_{j,t}^{m_i}}{\Delta f_{j,2^k t}^{\text{SCIP}_s}}, \quad (19)$$

where we chose $k = 0, \dots, 3$, $t \in T = \{1, \dots, 2^{3-k}\}$. The measure (19) expresses the ratio between the gap of two solutions: the first solution is the proposed approach, using model m , trained on \mathbf{tr}_i , evaluated on instance \mathbf{ts}_j , and the gap is reported after t hours; the second solution is the one provided by the solver SCIP, using SB or RPC, and evaluated on the same instance \mathbf{ts}_j , and the gap is reported after $2^k t$ hours. The elongation factor 2^k bestows upon SCIP a better chance to find a lower gap. When not found, it would assert the capability of our approach. For example, when $k = 0$, the duality gap of each solution is reported at $\{1, 2, 4, 8\}$ to examine a contrast of the classifiers' performance against SCIP_s under *equal* time limits, denoted (1:1). When $k = 1$, the gap is reported at $\{1, 2, 4\}$ and $\{2, 4, 8\}$, which yields a comparison of performance with *twice* the time limit for SCIP_s , denoted (1:2). Two further comparisons are made at (1:4) and (1:8), where $k = 2$ and $k = 3$, respectively, to determine if even larger gains are achieved by increasing the time limit by *four* and *eight* times.

For example, when $k = 0$, the duality gap of each solution is reported at $\{1, 2, 4, 8\}$ to examine a contrast of the classifiers' performance against SCIP_s under *equal* time limits, denoted (1:1). When $k = 1$, we report the gap at $\{1, 2, 4\}$ and $\{2, 4, 8\}$,

which yields a comparison of performance with twice the time limit for SCIP_s , denoted (1:2). We include two further comparisons at (1:4) and (1:8), where $k = 2$ and $k = 3$, respectively, to determine if our approach can achieve higher gains by increasing the time limit by four and eight times for SCIP_s .

We evaluate the average performance of each classifier in two ways: (1) by fixing the training instances and calculating the mean performance of *each* time-window comparison as previously described across the evaluation instances, using the following equation:

$$\Delta f_{\text{SCIP}_s}^m(i, t, k) = \frac{1}{|\mathbf{ts}|} \sum_{j \in \mathbf{ts}} \Delta f_{\text{SCIP}_s}^m(i, j, t, k). \quad (20)$$

(2) by averaging the performance across both the training and evaluation instances using the following equation (i.e., reduction by i and j):

$$\Delta f_{\text{SCIP}_s}^m(t, k) = \frac{1}{|\mathbf{tr}|} \sum_{i \in \mathbf{tr}} \Delta f_{\text{SCIP}_s}^m(i, t, k). \quad (21)$$

We also report two more measures to assess the aptitude of the classifiers to generalize in performance to larger and more complex instances, which are the GED and TSE. The GED is the number of edits required to make the topology of a graph \mathbf{tr}_i isomorphic to the topology of a graph \mathbf{ts}_j . The GED provides insights into the topological similarities between instances i and j . SCIP calculates the TSE as the relative increase in nodes between two consecutive tree states among all explored paths. The TSE of a classifier m trained on instance i and used as a branching strategy to solve evaluation instance j for t hours is denoted as $\text{TSE}_{j,t}^{m_i}$, while the TSE of the standard branching strategy s is denoted as $\text{TSE}_{j,t}^{\text{SCIP}_s}$. The ratio between these two quantities calculates how many more nodes the learned strategy needs to explore on larger instances compared to the standard one, s :


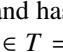
$$\Delta \text{TSE}_{\text{SCIP}_s}^{m_i} = \frac{1}{|T|} \sum_t \left(\frac{\text{TSE}_{j,t}^{m_i}}{\text{TSE}_{j,t}^{\text{SCIP}_s}} \right) \quad (22)$$

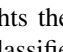
In Section 6, we normalized the displayed values of both the GED and $\Delta \text{TSE}_{\text{SCIP}_s}^m$ to the interval $[0, 1]$ for convenience.

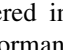
6. Results

We present the optimality gain described by (19) in Figures 8 and 9 for the CVRP and Figures 12 and 13 for the BPP. Since the four figures encompass the same elements. We will only describe the elements of Figures 8 and 9 and convey the same theme to the ones for the BPP. Each of Figures 8 and 9, which details the comparison against SCIP_{SB} and SCIP_{RPC} , comprises six rows for the training instances and three columns for the classifiers. We will use the notation $\text{Fig}(s, m, i)$ to refer to the figure describing the results of classifier m when trained on instance i and evaluated against SCIP_s on all instances \mathbf{ts} ; e.g., $\text{Fig}(\text{RPC}, \text{GCNN}, \text{A-n32-k5})$ is the top and leftmost sub-figure in Figure 9, representing the performance gain of GCNN when

trained on Instance A-n32-k5 and compared against SCIP_{RPC} . Each $\text{Fig}(s, m, i)$ has eight interior columns, one for each \mathbf{ts}_j , denoted $\text{Fig}(s, m, i, j)$; each is a lump of *four* distinctive gray-level bars to *visually* differentiate the four elongation factors 2^k defined in (19), and each is denoted $\text{Fig}(s, m, i, j, k)$.

For example, the first bar  is $\text{Fig}(s, m, i, j, 0)$ and has four symbols $- + \square \circ$ to represent $\Delta f_{\text{SCIP}_s}^m(i, j, t, 0)$ at $t \in T = \{1, \dots, 2^3\}$. That is, a performance ratio of the learned branching strategies to the standard ones when both are given equal time limits, which are 1, 2, 4, and 8 hours. The second bar  is $\text{Fig}(s, m, i, j, 1)$ and has three symbols $+ \square \circ$ to represent $\Delta f_{\text{SCIP}_s}^m(i, j, t, 1)$ at $t \in T = \{1, \dots, 2^2\}$. The other two bars follow a similar pattern for the remaining fourfold (1:4) and eightfold (1:8) time limit extensions for SCIP_s . In a limited number of experiments, SCIP_s fails to obtain a feasible solution in a certain time limit t on an evaluation instance j ; we distinguish those observations by using the same symbols as described previously, however, capped by an Ω , e.g., $\overset{\Omega}{-}$ and $\overset{\Omega}{+}$, and shifted to the top of the bar $\text{Fig}(s, m, i, j, k)$. A single Ω spanning the entire column $\text{Fig}(s, m, i, j)$ indicates the same meaning across the different values of k , and accordingly, t .

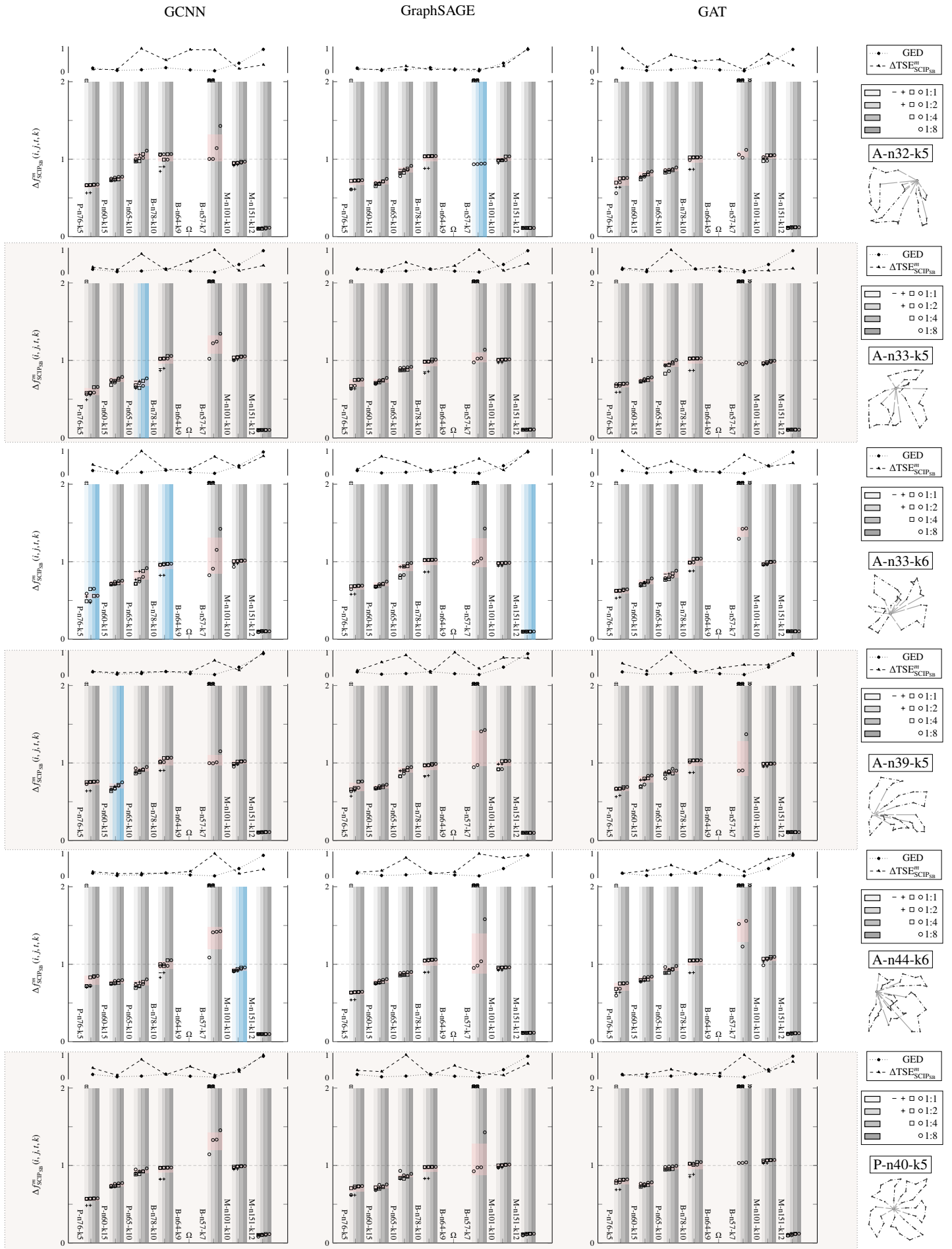
Equivalently, we use a flipped \cup to designate the similar behavior for a classifier m . Additionally, for each $\text{Fig}(s, m, i)$, there are two stacked lines on the top: the dotted line shows the topological *complexity* of each evaluation instance relatively to the training instance, computed by the GED; the triangle-dashed line reflects the $\Delta \text{TSE}_{\text{SCIP}_s}^{m_i}$ (22). The pale-red area height in $\text{Fig}(s, m, i, j)$, , highlights the standard deviation of the average gains achieved by classifier m trained on instance j against SCIP_s over the different values k

If a $\text{Fig}(s, m, i, j)$ is rendered in light blue color, , it indicates the highest performance gain when solving instance j using classifier m trained on instance i against SCIP_s , e.g., $\text{Fig}(\text{RPC}, \text{GCNN}, \text{A-n33-k5}, \text{P-n65-k10})$. The dashed line, $---$, fixed at $\Delta f_{\text{SCIP}_s}^m(i, j, t, k) = 1$ in a $\text{Fig}(s, m, i)$ separates the results into two segments. The area below the line is of particular interest because it is the region where the performance of a classifier m trained on instance i is equal to or better than that of SCIP_s for all instance $j \in \mathbf{ts}$.

6.1. Findings

6.1.1. CVRP

When examining Figure 8, which displays the classifiers' performance compared to SCIP_{SB} , it is visible that the trained classifiers outperform SCIP_{SB} in most experiments. They either meet or improve upon SCIP_{SB} 's performance, as indicated by the dashed line representing equal performance. These improvements are most palpable in $\text{Fig}(\text{SB}, \text{GCNN}, \text{A-n33-k6}, \text{P-n76-k5})$ and Figure (SB, GraphSAGE, A-n33-k6, M-n151-k12). Additionally, SCIP_{SB} was unable to find a feasible solution within the first hour for Instance P-n76-k5, as shown in $\text{Fig}(\text{SB}, m, i, \text{P-n76-k5}, 0)$, or within the first, second, and fourth hour for Instance B-n57-k7, as shown in $\text{Fig}(\text{SB}, m, i, \text{B-n57-k7}, 0)$. This trend continues for Instance B-n64-k9 across all time windows, as indicated by the Ω symbol. No-



10
Figure 8: The performance of the three CVRP classifiers against SCIPSB calculated by (19), across the training instances.

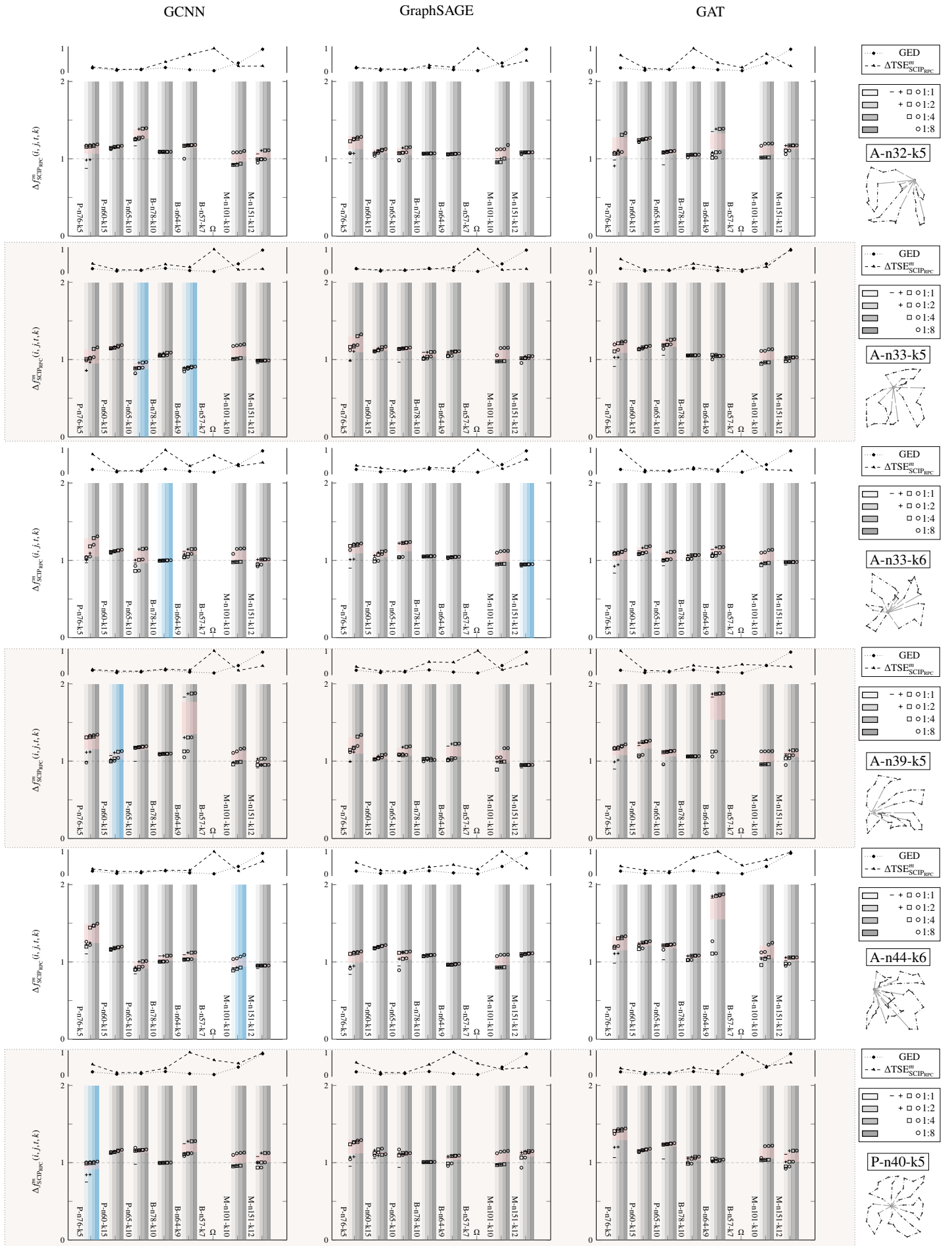


Figure 9: The performance of the three CVRP classifiers against SCIPRPC calculated by (19), across the training instances.

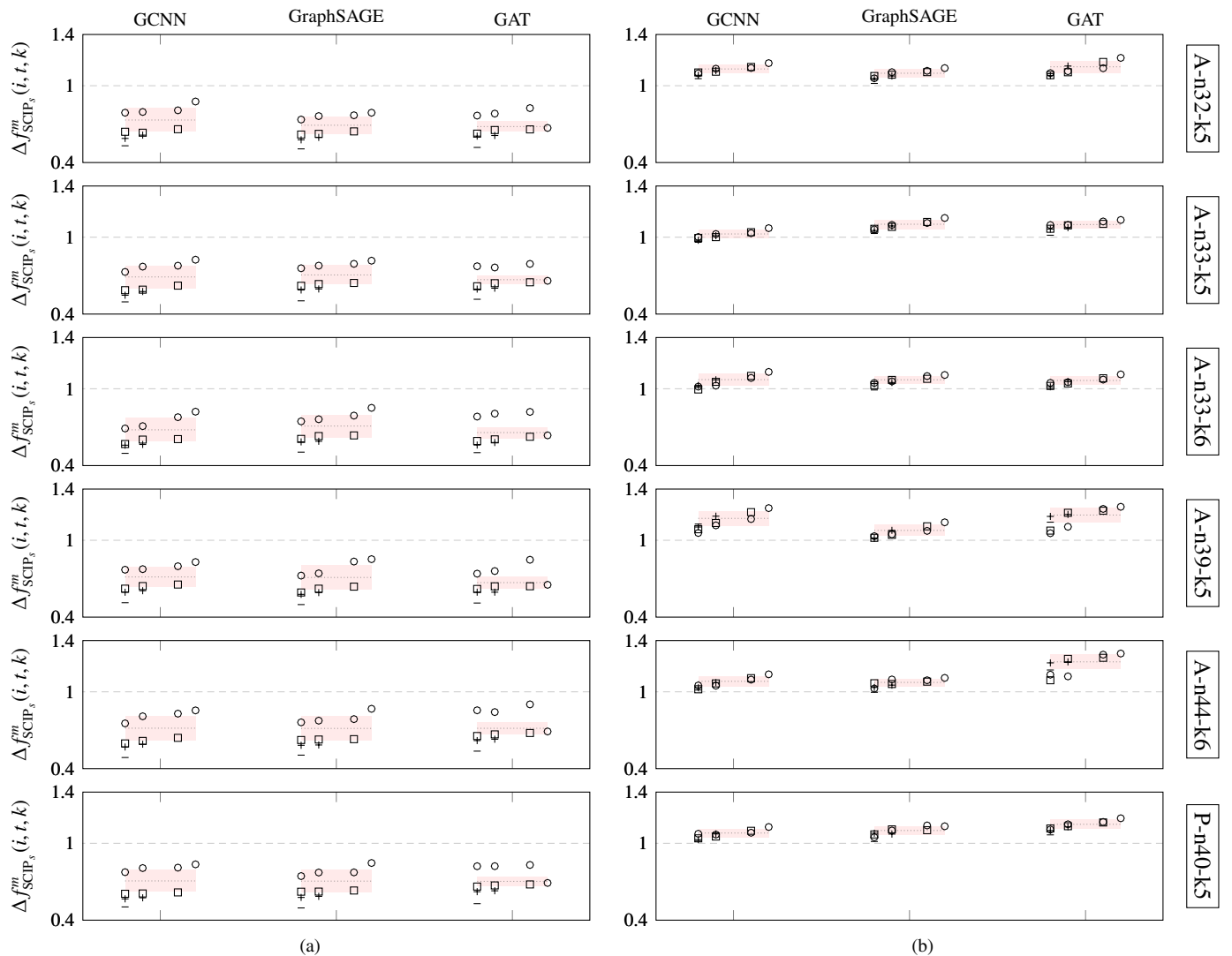


Figure 10: The average performance of each classifier across the CVRP evaluation instances: (a) compares against SCIP_{SB} and (b) compares against SCIP_{RPC} .

tably, the three classifiers find significantly lower gaps on Instance M-n151-k12, even when given the maximum time allowance to SCIP_{SB} (i.e., eight hours). Unfortunately, the GED and $\Delta\text{TSE}^m_{\text{SCIP}_{\text{SB}}}$ showed fluctuations with no apparent correlation to the classifiers' performance, making it challenging to affirm generalization capabilities. When comparing the performance of the individual classifiers, GCNN achieves the lowest gap in four out of eight instances; when compared to GraphSAGE, the surplus is, however, modest. GAT is able to outperform the other two classifiers at the eighth hour, which the average-performance figures emphasize. It is also worth mentioning that the classifiers trained on Instance A-n33-k6 found the lowest gap on Instances P-n76-k5, B-n78-k10, and M-n151-k12, which we attribute to a possible similarity of the complexity among them.

The classifiers' performance gains are also reflected in Figure 9, comparing against SCIP_{RPC} . Using the RPC strategy improves SCIP's performance. Nonetheless, at least one of the classifiers achieves equivalent performance with slight im-

provement or decline in at least four hours less. The GCNN remains the top-performing classifier on five out of eight evaluation instances. The number of the explored nodes is significantly smaller than those of SCIP_{RPC} , this is illustrated the triangle-dashed line representing the value of $\Delta\text{TSE}^m_{\text{SCIP}_{\text{RPC}}}$. The fourth bar \blacksquare shows particularly intriguing results, depicting the performance of the classifiers against a time allowance of an eightfold increase for SCIP_s . The potential gains when using the standard branching strategy are minute, and in some cases, there might be a net loss, which might not be worthwhile in time-critical sectors. On average, the classifiers consistently find lower gaps than SCIP_{SB} in considerably less time, as depicted in Figure 10a, which is calculated using (20). Although SCIP_{RPC} improves upon SCIP_{SB} 's performance as depicted in Figure 10b, the classifiers still exhibit impressive time savings. We further support these conclusions by Figure 11, which is calculated using (21), demonstrating the classifiers' capability

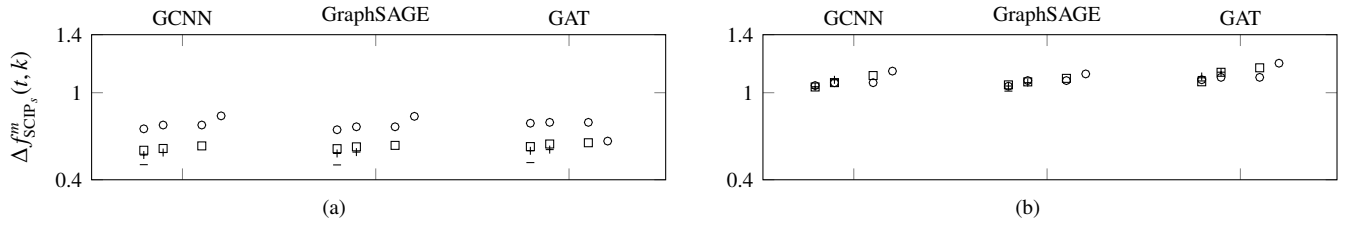


Figure 11: The performance of each classifier averaged by both of the CVRP training and evaluation instances against (a) $SCIP_{SB}$ and (b) $SCIP_{RPC}$.

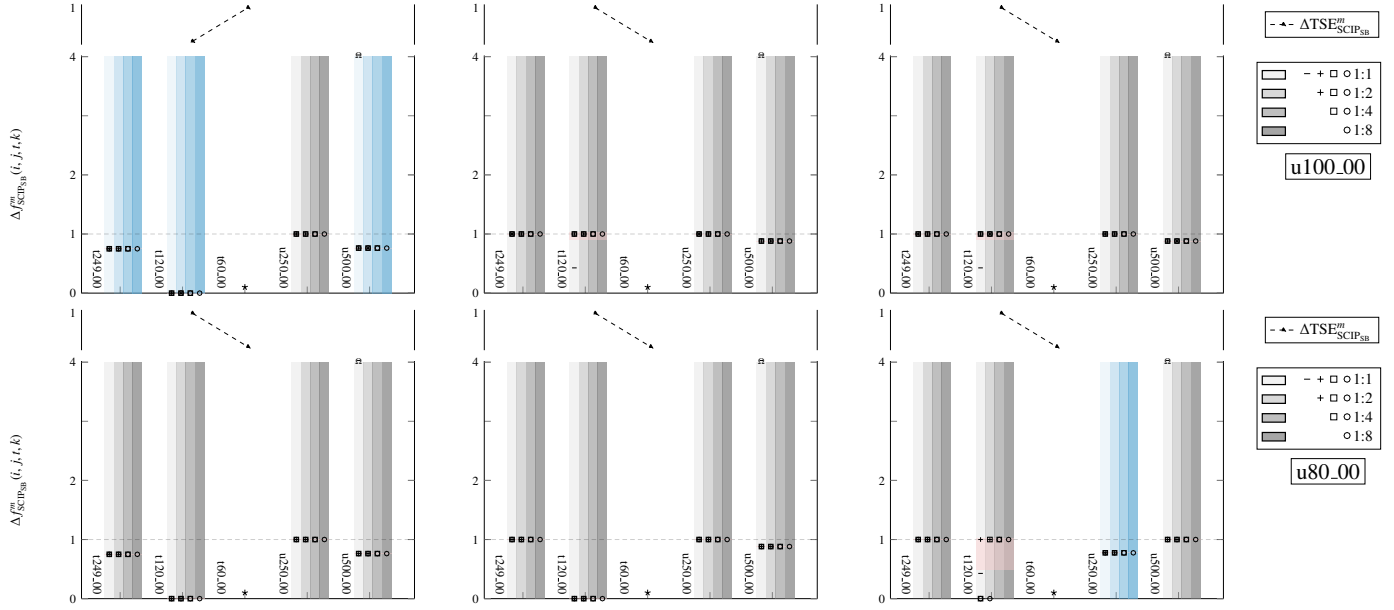


Figure 12: The performance of the three BPP classifiers against $SCIP_{SB}$ calculated by (19), across the training instances.

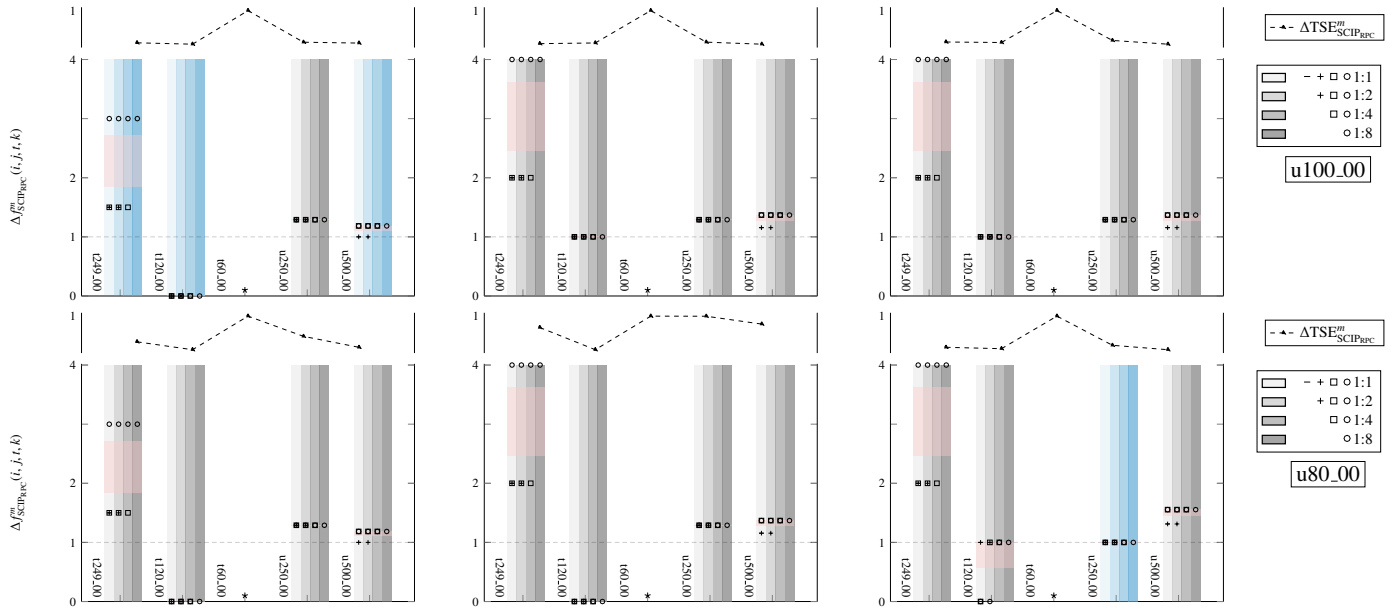


Figure 13: The performance of the three BPP classifiers against $SCIP_{RPC}$ calculated by (19), across the training instances.

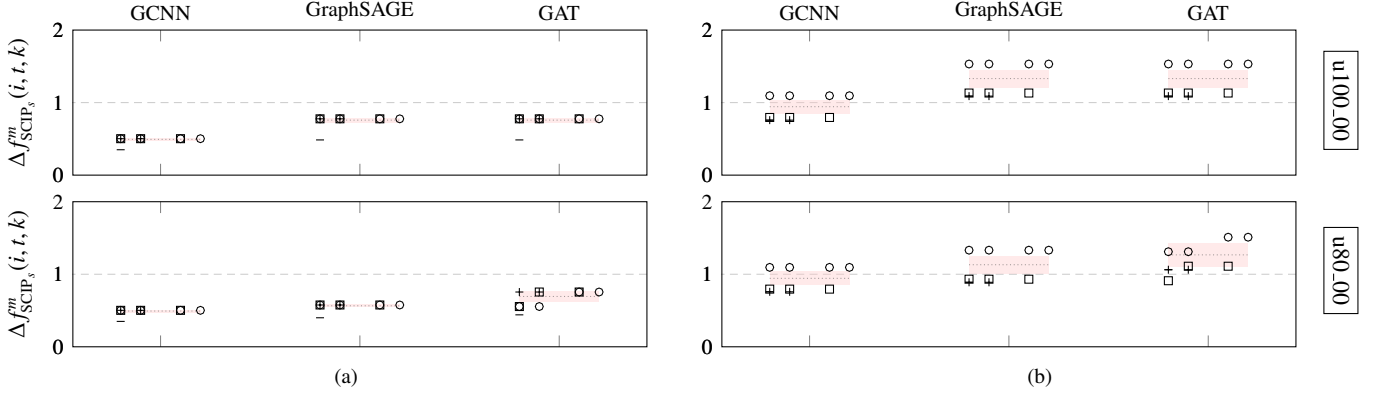


Figure 14: The average performance of each classifier across the BPP evaluation instances; (a) compares against SCIP_{SB} and (b) compares against SCIP_{RPC} .

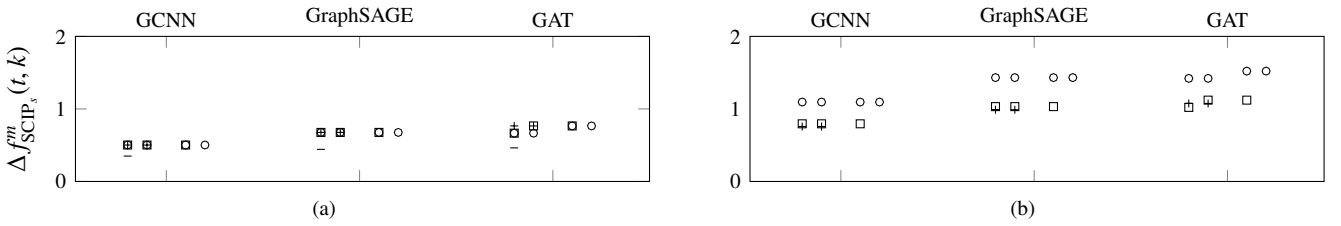


Figure 15: The performance of each classifier averaged by both of the BPP training and evaluation instances against (a) SCIP_{SB} and (b) SCIP_{RPC} .

to generalize to supposedly more complex instances². However, we refrain from using this observation as a response to the research question (C), given the unconfirmed correlation of the $\Delta \text{TSE}_{\text{SCIP}_s}^m$ or the GED with the classifiers' obtained gap.

6.1.2. BPP

Similar improvements against SCIP_{SB} are apparent in Figure 12. However, we noticed a pattern change; for example, the extended time limit no longer allows for further duality gap optimization, either for SCIP_{SB} or for classifier m_i , which we observed by the consistent values of $\Delta f_{\text{SCIP}_s}^m(i, j, t, k)$ across varying values of k . This is also asserted by the absence of tree-size estimates for three out of five evaluation datasets: t249_00, u250_00, and u500_00, due to the stagnant state of the search tree. We suspect that this is due to obtaining suboptimal distribution of items to bins within a limited time frame and that more time would be required to find improved solutions. Nonetheless, both SCIP_{SB} and the classifiers solved dataset t60_00 optimally; however, SCIP_{SB} failed to find a feasible solution for dataset t120_00. In Figure 13, SCIP_{RPC} appears to have an advantage on larger time windows for dataset t249_00, with a significantly lower gap than that of any of the classifiers. It also successfully obtains a feasible solution for dataset t120_00, albeit with a performance lead over the classifiers, which have solved the problem optimally. All of SCIP_{SB} and SCIP_{RPC} , as well as GCNN, GraphSAGE, and GAT, found optimal solutions for dataset t60_00 within the first hour. On average, the classifiers consistently achieve lower gaps than SCIP_{SB}

and show comparable performance to SCIP_{RPC} , as shown in Figures 14 through 15. It is also worth noting that variations in the training instances have minimal impact on the quality of the obtained solutions.

7. Conclusion

Our study underscores the potential of three geometric deep neural networks—graph convolutional neural network, GraphSAGE, and graph attention network—to either surpass or closely match the performance of the Strong Branching strategy in tackling the intricacies of the capacitated vehicle routing problem (CVRP) and bin packing problem. These classifiers exhibit minimal generalization error when confronted with new and more complex instances. Nonetheless, it is apparent that the existing literature lacks comprehensive metrics for accurately assessing the complexity of integer programs, a challenge attributed to their inherent intricacies.

While our findings are encouraging, they also point to challenges when dealing with larger instances with a significant number of customers. These challenges encompass issues related to generating decision samples for effective SB training of custom classifiers, as well as the current approach's limitations in devising strategies that surpass those it was trained on. To address these gaps, we propose two potential directions:

Firstly, leveraging the capabilities of UG (Shinano et al. 2012), a parallelized implementation of SCIP, that offers a promising avenue for refining our sampling tools. Additionally, initializing the training process with learned weights from smaller CVRP instances or different problem domains could

²We excluded the instances that SCIP_s was unable to find a feasible solution for.

potentially enhance classifier accuracy and efficiency when applied to larger instances.

Secondly, our ongoing work centers on reimagining the CVRP as a hide-and-seek game (J. von Neumann and Morgenstern 1947; John von Neumann 1953) involving two reinforcement-learning agents. In this paradigm, the objective is to maximize the *negative* relative primal-dual gap (Bichler et al. 2021). This approach involves one agent representing "hiding" elements (analogous to customers) and another agent as the "seeker" (equivalent to vehicles) in the pursuit of optimal solutions. The quality of the training set is no longer a limitation on this method.

In conclusion, this study uncovers promising avenues for the application of deep neural networks in addressing complex combinatorial optimization challenges, while also highlighting the need for further research in refining and expanding these approaches for substantial cases.

8. Acknowledgment

We express our gratitude for the partial support extended through the National Research Council of Canada's Artificial Intelligence for Logistics Program under Grant A-0035517. Furthermore, we acknowledge the contribution of the Digital Research Alliance of Canada for providing us with the computing hardware essential for the execution of our experiments. Thanks are also due to Brendan O'Donoghue for his valuable suggestions during the research process.

References

- Abu-Aisheh, Zeina et al. (Jan. 2015). "An Exact Graph Edit Distance Algorithm for Solving Pattern Recognition Problems". In: *4th International Conference on Pattern Recognition Applications and Methods 2015*. Lisbon, Portugal. doi: 10.5220/0005209202710278. URL: <https://hal.archives-ouvertes.fr/hal-01168816>.
- Achterberg, Tobias, Thorsten Koch, and Alexander Martin (2005). "Branching rules revisited". In: *Operations Research Letters* 33.1, pp. 42–54. ISSN: 0167-6377. doi: <https://doi.org/10.1016/j.orl.2004.04.002>. URL: <https://www.sciencedirect.com/science/article/pii/S0167637704000501>.
- Applegate, D. et al. (1995). *Finding Cuts in the TSP (A Preliminary Report)*. Tech. rep.
- Arora, Sanjeev and Boaz Barak (2009). "PCP theorem and hardness of approximation: An introduction". In: *Computational Complexity: A Modern Approach*. Cambridge University Press, pp. 237–256. doi: 10.1017/CB09780511804090.014.
- Ba, Jimmy Lei, Jamie Ryan Kiros, and Geoffrey E. Hinton (2016). *Layer Normalization*. doi: 10.48550/ARXIV.1607.06450. URL: <https://arxiv.org/abs/1607.06450>.
- Beasley, John E. (2004). *Operation Research Library*. URL: <http://people.brunel.ac.uk/~mastjjb/jeb/orlib/files/>.
- Bellman, Richard (Jan. 1962). "Dynamic Programming Treatment of the Travelling Salesman Problem". In: *J. ACM* 9.1, pp. 61–63. ISSN: 0004-5411. doi: 10.1145/321105.321111. URL: <https://doi.org/10.1145/321105.321111>.
- Bello, Irwan et al. (2016). "Neural Combinatorial Optimization with Reinforcement Learning". In: *CoRR* abs/1611.09940. arXiv: 1611.09940. URL: <http://arxiv.org/abs/1611.09940>.
- Bengio, Yoshua, Andrea Lodi, and Antoine Prouvost (2021). "Machine learning for combinatorial optimization: A methodological tour d'horizon". In: *European Journal of Operational Research* 290.2, pp. 405–421. ISSN: 0377-2217. doi: <https://doi.org/10.1016/j.ejor.2020.07.063>. URL: <https://www.sciencedirect.com/science/article/pii/S0377221720306895>.
- Bestuzheva, Ksenia et al. (Dec. 2021). *The SCIP Optimization Suite 8.0*. ZIB-Report 21-41. Zuse Institute Berlin. URL: <http://nbn-resolving.de/urn:nbn:de:0297-zib-85309>.
- Bichler, Martin et al. (Aug. 2021). "Learning equilibria in symmetric auction games using artificial neural networks". In: *Nature Machine Intelligence* 3.8, pp. 687–695. ISSN: 2522-5839. doi: 10.1038/s42256-021-00365-4. URL: <https://doi.org/10.1038/s42256-021-00365-4>.
- Boyd, Stephen et al. (Jan. 2011). "Distributed Optimization and Statistical Learning via the Alternating Direction Method of Multipliers". In: *Found. Trends Mach. Learn.* 3.1, pp. 1–122. ISSN: 1935-8237. doi: 10.1561/22000000016. URL: <https://doi.org/10.1561/22000000016>.
- Boyd, Stephen P. (2004 - 2004). *Convex optimization*. eng. Cambridge, UK: Cambridge University Press. Chap. 5, pp. 216–249. ISBN: 0521833787.
- Clarke, G. and J. W. Wright (Aug. 1964). "Scheduling of Vehicles from a Central Depot to a Number of Delivery Points". In: *Operations Research* 12.4, pp. 568–581. doi: 10.1287/opre.12.4.568. URL: <https://ideas.repec.org/a/inm/oropre/v12y1964i4p568-581.html>.
- Cornuéjols, Gérard, Miroslav Karamanov, and Yanjun Li (2006). "Early Estimates of the Size of Branch-and-Bound Trees". In: *INFORMS Journal on Computing* 18.1, pp. 86–96. doi: 10.1287/ijoc.1040.0107. eprint: <https://doi.org/10.1287/ijoc.1040.0107>. URL: <https://doi.org/10.1287/ijoc.1040.0107>.
- Dantzig, G. B. and J. H. Ramser (1959). "The Truck Dispatching Problem". In: *Management Science* 6.1, pp. 80–91. ISSN: 00251909, 15265501. URL: <http://www.jstor.org/stable/2627477> (visited on 07/30/2022).
- Feldman, Vitaly, Roy Frostig, and Moritz Hardt (2019). "The advantages of multiple classes for reducing overfitting from test set reuse". In: *CoRR* abs/1905.10360. arXiv: 1905.10360. URL: <http://arxiv.org/abs/1905.10360>.
- Gasse, Maxime et al. (2019). "Exact Combinatorial Optimization with Graph Convolutional Neural Networks". In: *CoRR* abs/1906.01629. arXiv: 1906.01629. URL: <http://arxiv.org/abs/1906.01629>.
- Ghaziri, Hassan (1996). "Supervision in the Self-Organizing Feature Map: Application to the Vehicle Routing Problem".

- lem”. In: *Meta-Heuristics: Theory and Applications*. Ed. by Ibrahim H. Osman and James P. Kelly. Boston, MA: Springer US, pp. 651–660. ISBN: 978-1-4613-1361-8. DOI: [10.1007/978-1-4613-1361-8_39](https://doi.org/10.1007/978-1-4613-1361-8_39). URL: https://doi.org/10.1007/978-1-4613-1361-8_39.
- Gillett, Billy E. and Leland R. Miller (1974). “A Heuristic Algorithm for the Vehicle-Dispatch Problem”. In: *Operations Research* 22.2, pp. 340–349. URL: <https://EconPapers.repec.org/RePEc:inm:oropre:v:22:y:1974:i:2:p:340-349>.
- Gupta, Prateek et al. (2020). “Hybrid models for learning to branch”. In: *Advances in neural information processing systems* 33, pp. 18087–18097.
- Hamilton, William L. (2020). “The Graph Neural Network Model”. In: *Graph Representation Learning*. Cham: Springer International Publishing, pp. 51–70. ISBN: 978-3-031-01588-5. DOI: [10.1007/978-3-031-01588-5_5](https://doi.org/10.1007/978-3-031-01588-5_5). URL: https://doi.org/10.1007/978-3-031-01588-5_5.
- Hamilton, William L., Rex Ying, and Jure Leskovec (2017). “Inductive Representation Learning on Large Graphs”. In: *CoRR* abs/1706.02216. arXiv: [1706.02216](https://arxiv.org/abs/1706.02216). URL: <http://arxiv.org/abs/1706.02216>.
- Hastie, Trevor, Robert Tibshirani, and Jerome Friedman (2009). “Model Assessment and Selection”. In: *The Elements of Statistical Learning: Data Mining, Inference, and Prediction*. New York, NY: Springer New York, pp. 219–259. ISBN: 978-0-387-84858-7. DOI: [10.1007/978-0-387-84858-7_7](https://doi.org/10.1007/978-0-387-84858-7_7). URL: https://doi.org/10.1007/978-0-387-84858-7_7.
- Hendel, Gregor et al. (2022). “Estimating the Size of Branch-and-Bound Trees”. In: *INFORMS Journal on Computing* 34.2, pp. 934–952. DOI: [10.1287/ijoc.2021.1103](https://doi.org/10.1287/ijoc.2021.1103). URL: <https://doi.org/10.1287/ijoc.2021.1103>.
- Ho, Yu-Chi and D.L. Pepyne (2001). “Simple explanation of the no free lunch theorem of optimization”. In: *Proceedings of the 40th IEEE Conference on Decision and Control (Cat. No.01CH37228)*. Vol. 5, 4409–4414 vol.5. DOI: [10.1109/CDC.2001.980896](https://doi.org/10.1109/CDC.2001.980896).
- Hopfield, J. J. and D. W. Tank (July 1985). ““Neural” computation of decisions in optimization problems”. In: *Biological Cybernetics* 52.3, pp. 141–152. ISSN: 1432-0770. DOI: [10.1007/BF00339943](https://doi.org/10.1007/BF00339943). URL: <https://doi.org/10.1007/BF00339943>.
- Khalil, Elias et al. (Feb. 2016). “Learning to Branch in Mixed Integer Programming”. In: *Proceedings of the AAAI Conference on Artificial Intelligence* 30.1. DOI: [10.1609/aaai.v30i1.10080](https://ojs.aaai.org/index.php/AAAI/article/view/10080). URL: <https://ojs.aaai.org/index.php/AAAI/article/view/10080>.
- Kingma, Diederik P. and Jimmy Ba (2014). *Adam: A Method for Stochastic Optimization*. DOI: [10.48550/ARXIV.1412.6980](https://arxiv.org/abs/1412.6980). URL: <https://arxiv.org/abs/1412.6980>.
- Kool, Wouter, Herke van Hoof, and Max Welling (Mar. 2018). “Attention, Learn to Solve Routing Problems!” In: *arXiv e-prints*, arXiv:1803.08475, arXiv:1803.08475. arXiv: [1803.08475](https://arxiv.org/abs/1803.08475) [stat.ML].
- Land, A. H. and A. G. Doig (1960). “An Automatic Method of Solving Discrete Programming Problems”. In: *Econometrica* 28.3, pp. 497–520. ISSN: 00129682, 14680262. URL: <http://www.jstor.org/stable/1910129> (visited on 08/09/2022).
- Lenstra, J. K. and A. H. G. Rinnooy Kan (1981). “Complexity of vehicle routing and scheduling problems”. In: *Networks* 11.2, pp. 221–227. DOI: <https://doi.org/10.1002/net.3230110211>. eprint: <https://onlinelibrary.wiley.com/doi/pdf/10.1002/net.3230110211>. URL: <https://onlinelibrary.wiley.com/doi/abs/10.1002/net.3230110211>.
- Lima, Ivan et al. (2014). *Capacitated Vehicle Routing Problem Library*. URL: <http://vrp.galgos.inf.puc-rio.br/>.
- Lipton, R. J. and K. W. Regan (2012). *Branch And Bound—Why Does It Work*. URL: <https://rjlipton.wpcomstaging.com/2012/12/19/branch-and-bound-why-does-it-work/> (visited on 12/19/2012).
- Mania, Horia et al. (2019). “Model Similarity Mitigates Test Set Overuse”. In: *Advances in Neural Information Processing Systems*. Ed. by H. Wallach et al. Vol. 32. Curran Associates, Inc. URL: <https://proceedings.neurips.cc/paper/2019/file/48237d9f2dea8c74c2a72126cf63d933-Paper.pdf>.
- Martello, Silvano and Paolo Toth (1990). *Knapsack Problems: Algorithms and Computer Implementations*. USA: John Wiley & Sons, Inc., pp. 221–240. ISBN: 0471924202.
- Miller, C. E., A. W. Tucker, and R. A. Zemlin (Oct. 1960). “Integer Programming Formulation of Traveling Salesman Problems”. In: *J. ACM* 7.4, pp. 326–329. ISSN: 0004-5411. DOI: [10.1145/321043.321046](https://doi.org/10.1145/321043.321046). URL: <https://doi.org/10.1145/321043.321046>.
- Morrison, David R. et al. (2016). “Branch-and-bound algorithms: A survey of recent advances in searching, branching, and pruning”. In: *Discrete Optimization* 19, pp. 79–102. ISSN: 1572-5286. DOI: <https://doi.org/10.1016/j.disopt.2016.01.005>. URL: <https://www.sciencedirect.com/science/article/pii/S1572528616000062>.
- Nair, Vinod et al. (2020). “Solving mixed integer programs using neural networks”. In: *arXiv preprint arXiv:2012.13349*.
- Nazari, MohammadReza et al. (2018). “Reinforcement Learning for Solving the Vehicle Routing Problem”. In: *Advances in Neural Information Processing Systems*. Ed. by S. Bengio et al. Vol. 31. Curran Associates, Inc. URL: <https://proceedings.neurips.cc/paper/2018/file/9fb4651c05b2ed70fba5afe0b039a550-Paper.pdf>.
- Neumann, J. von and O. Morgenstern (1947). “ZERO-SUM GAMES : THEORY”. In: *Theory of Games and Economic Behavior*. Princeton University Press, pp. 85–165.
- Neumann, John von (1953). “1. A Certain Zero-sum Two-person Game Equivalent to the Optimal Assignment Problem”. In: *Contributions to the Theory of Games (AM-28), Volume II*. Ed. by Harold William Kuhn and Albert William Tucker. Princeton: Princeton University Press, pp. 5–12. ISBN: 9781400881970. DOI: [doi:10.1515/9781400881970-002](https://doi.org/10.1515/9781400881970-002). URL: <https://doi.org/10.1515/9781400881970-002>.
- Özaltın, Osman Y., Brady Hunsaker, and Andrew J. Schaefer (2011). “Predicting the Solution Time of Branch-and-Bound Algorithms for Mixed-Integer Programs”. In: *IN-*

- FORMS Journal on Computing* 23.3, pp. 392–403. doi: [10.1287/ijoc.1100.0405](https://doi.org/10.1287/ijoc.1100.0405). eprint: <https://doi.org/10.1287/ijoc.1100.0405>. URL: <https://doi.org/10.1287/ijoc.1100.0405>.
- P, Augerat. et al. (Sept. 1995). *Computational results with a branch and cut code for the capacitated vehicle routing problem*.
- , paolo toth paolo and danielle vigo danielle (2002). *the vehicle routing problem*. Ed. by paolo toth and danielle vigo. society for industrial and applied mathematics. doi: [10.1137/1.9780898718515](https://doi.org/10.1137/1.9780898718515). eprint: <https://epubs.siam.org/doi/pdf/10.1137/1.9780898718515>. URL: <https://epubs.siam.org/doi/abs/10.1137/1.9780898718515>.
- Papadimitriou, Christos and Mihalis Yannakakis (1988). “Optimization, Approximation, and Complexity Classes”. In: *Proceedings of the Twentieth Annual ACM Symposium on Theory of Computing*. STOC ’88. Chicago, Illinois, USA: Association for Computing Machinery, pp. 229–234. ISBN: 0897912640. doi: [10.1145/62212.62233](https://doi.org/10.1145/62212.62233). URL: <https://doi.org/10.1145/62212.62233>.
- Pawitan, Y. (2013). In *All Likelihood: Statistical Modelling and Inference Using Likelihood*. In *All Likelihood: Statistical Modelling and Inference Using Likelihood*. OUP Oxford. Chap. 13. ISBN: 9780199671229. URL: <https://global.oup.com/academic/product/in-all-likelihood-9780199671229>.
- Prouvost, Antoine et al. (2020). “Ecole: A Gym-like Library for Machine Learning in Combinatorial Optimization Solvers”. In: *Learning Meets Combinatorial Algorithms at NeurIPS2020*. URL: <https://openreview.net/forum?id=IVc9hqqibyB>.
- Shinano, Yuji et al. (2012). “ParaSCIP: A Parallel Extension of SCIP”. In: *Competence in High Performance Computing 2010*. Ed. by Christian Bischof et al. Berlin, Heidelberg: Springer Berlin Heidelberg, pp. 135–148. ISBN: 978-3-642-24025-6.
- Sutton, Richard S. and Andrew G. Barto (2018). *Reinforcement Learning: An Introduction*. Cambridge, MA, USA: A Bradford Book. ISBN: 0262039249.
- Torki, Abdolhamid, Samerkae Somhon, and Takao Enkawa (1997). “A competitive neural network algorithm for solving vehicle routing problem”. In: *Computers & Industrial Engineering* 33.3. Selected Papers from the Proceedings of 1996 ICC&IC, pp. 473–476. ISSN: 0360-8352. doi: [https://doi.org/10.1016/S0360-8352\(97\)00171-X](https://doi.org/10.1016/S0360-8352(97)00171-X). URL: <https://www.sciencedirect.com/science/article/pii/S036083529700171X>.
- Uchoa, Eduardo et al. (2017). “New benchmark instances for the Capacitated Vehicle Routing Problem”. In: *European Journal of Operational Research* 257.3, pp. 845–858. ISSN: 0377-2217. doi: <https://doi.org/10.1016/j.ejor.2016.08.012>. URL: <https://www.sciencedirect.com/science/article/pii/S0377221716306270>.
- Veličković, Petar et al. (2017). *Graph Attention Networks*. doi: [10.48550/ARXIV.1710.10903](https://arxiv.org/abs/1710.10903). URL: <https://arxiv.org/abs/1710.10903>.
- Vinyals, Oriol, Meire Fortunato, and Navdeep Jaitly (2015). *Pointer Networks*. doi: [10.48550/ARXIV.1506.03134](https://arxiv.org/abs/1506.03134). URL: <https://arxiv.org/abs/1506.03134>.
- Wosley, Laurence (2020). “Complexity and Problem Reductions”. In: *Integer Programming*. John Wiley & Sons, Ltd. Chap. 7, pp. 123–129. ISBN: 9781119606475. doi: <https://doi.org/10.1002/9781119606475.ch6>. eprint: <https://onlinelibrary.wiley.com/doi/pdf/10.1002/9781119606475.ch6>. URL: <https://onlinelibrary.wiley.com/doi/abs/10.1002/9781119606475.ch6>.
- Zarpellon, Giulia et al. (2020). “Parameterizing Branch-and-Bound Search Trees to Learn Branching Policies”. In: *CoRR* abs/2002.05120. arXiv: 2002.05120. URL: <https://arxiv.org/abs/2002.05120>.